I&EC research
Industrial & Engineering Chemistry Research

pubs.acs.org/IECR
Article

Lyogel Equilibria with Helmholtz Equations of State. Part II: Assessment of PC-SAFT Parametrizations and Network Models for pNIPAM Lyogels

Published as part of Industrial & Engineering Chemistry Research special issue "Smart Reactors—Towards Adaptive, Resilient, and Autonomous Process Systems".

Nanning Jaeschke,* Walter G. Chapman,* and Irina Smirnova

Cite This: *Ind. Eng. Chem. Res.* 2026, 65, 16852−16866

ABSTRACT: This work investigates the equilibrium swelling of poly(*N*-isopropylacrylamide) (pNIPAM)-based lyogels in multicomponent solvent systems using a Perturbed-Chain Statistical Associating Fluid Theory (PC-SAFT)-based thermodynamic framework coupled with polymer-network elasticity. Literature parameter sets for the butyl esterification system were assessed and refined, and different network models were compared within a sequential fitting strategy that links solvent, polymer-solution, and gel data. The results show that the framework can reproduce key swelling trends and supports the transfer of calibrated network parameters between related solvent descriptions. At the same time, the study highlights important limitations: quantitative fitting of lower critical solution temperature (LCST) behavior requires a temperature-dependent interaction parameter, finite-extensibility effects are negligible for the investigated systems, and the transferability of fitted interaction parameters to mixed solvents is limited. Overall, the work provides a practical framework for gel-equilibrium calculations while emphasizing the need for careful interpretation of fitted parameters.

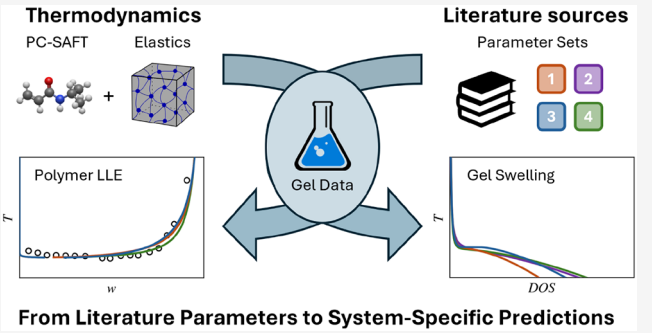

INTRODUCTION AND MOTIVATION

Smart materials have attracted growing attention because they combine sensing and actuation within a single material platform. Among them, stimuli-responsive polymers are of particular interest, as they undergo pronounced changes in response to external stimuli such as temperature,[1−3] solvent composition,[1−5] and pH.[6] Owing to these properties, such materials are increasingly being explored in both medical[7] and industrial applications.[8] In particular, recent progress in integrating responsive gels into smart reactor concepts,[9] including work within the German Collaborative Research Center SFB 1615 "SMART Reactors", highlights the need for reliable thermodynamic descriptions to support the design and operation of such systems under varying reaction conditions.

This work builds upon the methodology introduced in a previous contribution,[10] in which gels were modeled using state-of-the-art numerical algorithms for polymer-solution phase behavior[11−13] in combination with the PC-SAFT equation of state.[14,15] In the present study, this framework is applied to and further evaluated for the butyl esterification system. This system is a suitable case study because extensive data are available for the underlying solvent liquid−liquid equilibrium, including water, acetic acid, butanol, and butyl acetate. At the same time, it is of practical relevance and includes components that remain challenging for thermodynamic modeling, most notably acetic acid.

The polymer considered in this work is poly(*N*-isopropylacrylamide) (pNIPAM), a widely studied thermo-responsive polymer that forms gels with pronounced swelling behavior. This makes pNIPAM an attractive model system for assessing both the predictive capability of the thermodynamic approach and the robustness of the underlying numerical framework. Because the literature provides a range of parametrizations for the esterification system, three different parameter sets are examined in this study. This comparison is intended to assess the applicability of literature parametrizations and, together with the open-access code provided,[16] to clarify to what extent individual parameters can describe or explain the observed

Received: April 9, 2026
Revised: July 7, 2026
Accepted: July 9, 2026
Published: August 2, 2026

https://doi.org/10.1021/acs.iecr.6c01731
Ind. Eng. Chem. Res. 2026, 65, 16852−16866

effects. At the same time, the analysis highlights the transferability and limitations of such parameter sets.

In addition, the literature offers a variety of network models[17−19] each based on different assumptions and associated with specific advantages and limitations. The present work therefore compares the applicability of these models in a practically relevant case study and evaluates the extent to which they improve the description of gel behavior. More specifically, this study pursues three objectives: first, to assess literature PC-SAFT parameter sets for the butyl esterification system; second, to compare different network-model formulations for the description of gel swelling; and third, to evaluate the transferability and limitations of calibrated parameters across related systems. By combining thermodynamic modeling, numerical methodology, parameter assessment, and network-model comparison, this work aims to provide a practical and transparent framework for reliable gel-equilibrium calculations and thereby support the future design of smart material-based process systems.

THEORY

The theoretical foundation and methodology of the present work have been described in detail in a previous contribution.[10] In brief, the key assumption for gel equilibria is the elevated pressure inside the gel phase, which is accounted for by an elastic free energy contribution, A_{el}. Maurer and Prausnitz[20] demonstrated that this contribution can be incorporated into the equilibrium condition as

$$\mu_i'(T, p', \boldsymbol{n}') = \mu_i''(T, p', \boldsymbol{n}'') + \overline{v}_i'' \left.\frac{\partial A_{el}}{\partial V}\right|_{V''} \tag{1}$$

where the elastic term acts as a Poynting-like correction. μ_i' and μ_i'' denote the chemical potentials of component i in the external solvent phase and in the gel pseudophase, respectively, both evaluated at the ambient pressure p'; $\boldsymbol{n}'$ and $\boldsymbol{n}''$ are the corresponding vectors of mole numbers, $\overline{v}_i''$ is the partial molar volume of component i in the gel phase, and V'' is the gel volume. This formulation was subsequently integrated into a modified second-order polymer solution algorithm based on the approaches originally proposed by von Solms et al.,[12] Lindvig et al.,[11] and Michelsen and Mollerup.[13] In the present work, the PC-SAFT equation of state[14,15] is used as the underlying thermodynamic model.

Network Theories

A central aspect of gel modeling is the definition of a suitable expression for the network contribution. The literature provides extensive discussion on the applicability and physical justification of different network models.[21−24] The most prominent approaches are the affine network theory, developed by Flory and Rehner,[17,25,26] the phantom network theory, developed by James and Guth,[18,27−29] and the finite extensibility (FE) network theory, introduced by Miao et al.[19] Their elastic free energy contributions can be written as

$$\frac{A_{el}^{aff}}{k_B T} = n_{chain} C^{aff} \left\{ \frac{3}{2}\left[\left(\frac{V}{V_{ref}}\right)^{2/3} - 1\right] - \ln\frac{V}{V_{ref}} \right\} \tag{2}$$

$$\frac{A_{el}^{pht}}{k_B T} = n_{chain} C^{pht} \left\{ \frac{3}{2}\left[\left(\frac{V}{V_{ref}}\right)^{2/3} - 1\right] \right\} \tag{3}$$

$$\frac{A_{el}^{FE}}{k_B T} = n_{chain} C^{FE} \left\{ \frac{3}{2}\left[\left(\frac{V}{V_{ref}}\right)^{2/3} - 1\right]\left[1 - \left(\frac{V}{V_{max}}\right)^{2/3}\right]^{-1} - \ln\frac{V}{V_{ref}} \right\} \tag{4}$$

Here, n_{chain} denotes the number of elastically active network chains, C is the model-specific prefactor accounting for the assumed network topology and cross-link fluctuations, V is the current gel volume, V_{ref} is the reference volume, and V_{max} is the maximum volume introduced in the finite-extensibility model. These network theories were originally developed to describe the entropic elasticity of rubber-like materials, focusing on the deformation of a polymer network relative to a reference volume V_{ref}. In the literature, the reference volume is commonly chosen either as the dry polymer volume[30,31] or as the gel volume at the time of network formation.[1,20] The primary difference between the affine and phantom network models lies in their assumptions regarding the mobility of cross-links under macroscopic deformation.[24] Although both approaches lead to mathematically similar functional forms, they differ in the physical interpretation and magnitude of the prefactor C.[24,32]

Beyond the interpretation of C, the affine and phantom network theories also differ in their treatment of the logarithmic term, which has been associated with ideal-gas-like behavior of the network junctions.[26] Owing to extensive discussion in the literature,[28,29,33,34] a heterogeneous set of formulations has emerged. Although attempts have been made to reconcile these approaches[35,36] practical modeling studies most often treat the prefactor C as an adjustable parameter.[1,30−32,37−39] Consequently, the qualitative shape of the elastic free energy contribution is of primary relevance, as illustrated in Figure 1.

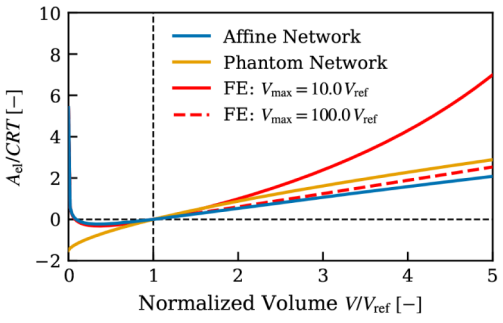

Figure 1. Elastic free energy scaled by C, A_{el}/CRT as a function of normalized volume V/V_{ref} for the considered affine, phantom, and finite-extensibility (FE) network models. The dashed line indicates a different value of the maximum extensibility V_{max} for the FE network model.

In the present work, both the affine and FE network theories are considered in formulations that include the logarithmic contribution, which introduces a repulsive term in the limit of small volumes. The reference volume defines the state at which the elastic free energy of the network vanishes, although this state does not necessarily coincide with the minimum of the free energy.

https://doi.org/10.1021/acs.iecr.6c01731
Ind. Eng. Chem. Res. 2026, 65, 16852−16866

Since the affine and phantom network theories were originally developed for relatively small deformations in rubber-like materials, Miao et al.[19] extended the affine network model to account for finite chain extensibility. This was achieved by introducing a mathematical singularity as the gel volume V approaches a maximum volume V_{max}. This maximum volume has been interpreted either as the theoretical limit of fully stretched chains,[19] for example in an ideal tetrahedral network[30,38,40] or as an additional fitting parameter.[31,41] As shown in Figure 1, the FE model coincides with the affine network model at moderate swelling and diverges only as the volume approaches V_{max}.

For the equilibrium calculations described by eq 1, the relevant quantity is not the elastic free energy itself, but its first volumetric derivative, $\partial A_{el}/\partial V$, which corresponds to the negative elastic pressure. This derivative is shown for the considered network models in Figure 2. Although the elastic

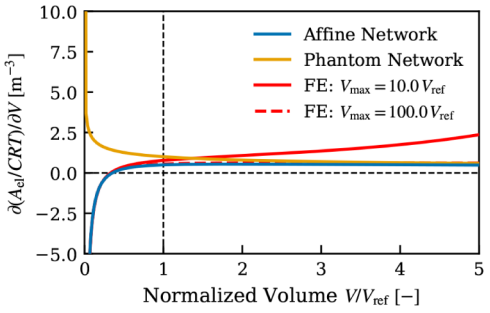

Figure 2. Volume derivative of the elastic free energy, $\partial A_{el}/\partial V$, as used in the equilibrium calculations for the considered network models. The dashed line indicates a different value of the maximum extensibility V_{max} for the FE network model.

free energy is zero at the reference volume V_{ref}, the elastic pressure is generally nonzero at this point and therefore shifts the equilibrium. In other words, the transition from an equilibrated polymer solution to an equilibrated gel leads to a shifted equilibrium state, even when the reference volume coincides with that of the current polymer solution.

At large volumes, both the affine and phantom network models approach vanishing elastic pressure. In contrast, the FE network model exhibits a diverging elastic pressure as the volume approaches V_{max}. For sufficiently large values of V_{max}, the FE model collapses onto the affine network model within the volume range shown and is therefore not distinguishable in Figure 2.

The elastic contribution can also be expressed in terms of the polymer volume fraction ϕ_{poly}, thereby linking the model to the experimentally accessible gel volumes V and V_{ref} through

$$\frac{\phi_{poly}^{ref}}{\phi_{poly}} = \frac{\overline{v}_{poly}^{ref} n_{poly}}{V_{ref}} \frac{V}{\overline{v}_{poly} n_{poly}} \approx \frac{V}{V_{ref}} \quad (5)$$

While the number of polymer molecules n_{poly} is, by definition, constant for a given gel specimen, the partial molar volume of the polymer $\overline{v}_{poly}$ may in principle differ between the reference state and the current state. In agreement with Maurer and Prausnitz,[20] this difference is neglected as an approximation.

METHODS

Pure-component PC-SAFT parameters were first compiled for all solvent components (see Table 1). The polymer-free solvent systems were then described using three literature parameter sets developed for esterification systems. In addition, a fourth water parametrization proposed by Arndt and Sadowski[30] for the pNIPAM−water system was considered. This parametrization was used as a reference to transfer the pNIPAM parameters reported by Arndt and Sadowski[30] to the remaining parameter sets, which were either developed for esterification reactions or adapted from related parametrizations.

Table 1. Pure-Component PC-SAFT Parameter Sources Used in the Different Parameter Sets[a]

Parameters	Arndt and Sadowski[30]	Esper et al.[44]	Jovein et al.[43]	Grob and Hasse[42]
Polymer (P)	X[30]			
Water (W)	X[46]	X[44]	X[46]	X[47]
Butanol (B)		X[44]	X[47]	X[47]
Butyl acetate (BA)		X[44]	X[48]	X[15,42]
Acetic acid (AA)		X[44]	X[47]	X[47]

[a]In all parameter sets, water, butanol, and acetic acid are represented with one donor and one acceptor site. The treatment of butyl acetate differs between parametrizations: it is modeled as non-associating by Jovein et al., with one donor and one acceptor site by Grob and Hasse, and with two acceptor sites and a polar moment by Esper et al.

The parameter set of Grob and Hasse[42] was developed specifically for the butyl esterification system, but was fitted to experimental data at higher temperatures (80−120 °C) than those considered here. The parameter set of Jovein et al.[43] compiles PC-SAFT parameters for a broader range of esterification reactions. In both cases, previously published pure-component parameters were adopted and selectively refined to improve agreement with experimental phase-equilibrium data.

The final parameter set used in this work combines the pure-component parametrizations of Esper et al.[44] with the binary interaction treatment proposed by Rehner et al.[45] Both sources provide PC-SAFT parameters for a broad range of components. Unlike the other approaches, Rehner et al.[45] optimized binary cross-association energy parameters ε_{ij}^{AB} whenever this gave better agreement with experimental data than adjustment of the binary dispersion interaction parameter k_{ij}.

For each parameter set, model performance was evaluated and binary interaction parameters were subsequently optimized. Experimental phase-equilibrium data were collected from the literature for systems exhibiting liquid−liquid miscibility gaps. An overview of the investigated pure, binary, and ternary systems is given in Table 2. After establishing an adequate description of the esterification system, polymer-containing systems were considered. For the non-crosslinked

Table 2. Experimental Literature Sources for Solvent, Polymer (P), and Gel (G) Systems[a]

System type	Solvent LLE sources	Polymeric LLE sources
Pure component	DIPPR[49]	-
Binary	W−B[50−52]	P−W[1,53−55]
	W−BA[50−52]	G−W[1,3,56,57]
Ternary	W−B−AA,[42,51,58]	G−W−AA[57]
	W−BA−AA,[42,51,58]	G−AA−BA[4]
	W−B−BA,[42,51,58]	G−BA−B[4]

[a]The polymer considered in this work is pNIPAM, and the solvents are abbreviated as water (W), butanol (B), butyl acetate (BA), and acetic acid (AA).

https://doi.org/10.1021/acs.iecr.6c01731
Ind. Eng. Chem. Res. 2026, 65, 16852−16866

polymer, only polymer−water LLE data were available. Swelling data for cross-linked gels were taken from several literature sources, also summarized in Table 2.

Parameter optimization was based on a cost function that emphasizes solubility data, which are generally more widely available than tie-line data, particularly for polymer and gel systems. Partition coefficients were not used, because polymer-containing systems often exhibit phases with negligible polymer content. In such cases, partition coefficients can become extremely large and numerically unstable, even though the experimentally observed solubility remains negligible.

The cost function was defined as the mean squared distance of each experimental point to the nearest of the two calculated binodal branches. In the ternary case, the experimental and calculated compositions $\mathbf{w} = (w_1,w_2,w_3)$ are mapped from ternary composition space into Cartesian coordinates according to

$$x = w_2 + \frac{1}{2}w_3 \tag{6}$$

$$y = \frac{\sqrt{3}}{2}w_3 \tag{7}$$

where the w_i are expressed in percent. In the binary case, the state point was represented directly in the two-dimensional space

$$\mathbf{x} = \left(\frac{T}{T_{\text{scale}}}, w_i\right) \tag{8}$$

where T denotes the temperature, T_{scale} = 1 K is the scaling temperature, and w_i the selected mass fraction in percent. The choice of T_{scale} = 1 K is inherently somewhat arbitrary. However, it yielded reasonable results. A sensitivity study on the influence of different T_{scale} values is provided in the Supporting Information. Denoting the experimental points by $\mathbf{x}_k$ and the two resampled calculated binodal branches by Γ_{I} and Γ_{II}, the binodal cost function was written as

$$J_{\text{binodal}} = \frac{1}{N}\sum_{k=1}^{N} \min(d^2(\mathbf{x}_k, \Gamma_{\text{I}}), d^2(\mathbf{x}_k, \Gamma_{\text{II}})) \tag{9}$$

where $d^2(\mathbf{x},\Gamma)$ denotes the squared Euclidean distance from point $\mathbf{x}$ to the polyline Γ. Thus, the ternary and binary cases differ only in the coordinate representation used for the comparison: ternary data are projected from composition space onto the triangular diagram, whereas binary data are compared directly in $(T/T_{\text{scale}}, w_i)$ space.

For swelling, or degree-of-swelling (DOS), data, the cost function was defined as the root-mean-square relative deviation between experimental DOS values and calculated DOS values for the given temperature and composition of the solvent phase. The calculated DOS was obtained from the gel phase branch according to

$$DOS^{\text{calc}} = \frac{1}{w_{\text{poly}}^{\text{gel}}} \tag{10}$$

and the corresponding DOS cost function for N experimental measurements was defined as

$$J_{DOS} = \sqrt{\frac{1}{N}\sum_{k=1}^{N}\left(\frac{DOS_k^{\text{calc}} - DOS_k^{\text{exp}}}{DOS_k^{\text{exp}}}\right)^2} \tag{11}$$

This results in a well-conditioned objective function that also captures critical and near-critical regions. This treatment is particularly important for pNIPAM and other LCST-type polymers, whose binodal typically exhibits a flat-bottomed shape with steep branches, causing experimentally determined cloud-point and demixing temperatures to cluster near the critical temperature. The resulting optimization problem was solved using a differential evolution algorithm.

To separate parameter estimation from model validation, all calculations were performed within a sequential fitting framework. Literature pure-component and binary parameters were adopted as fixed input wherever possible, while additional model parameters were adjusted only at the stage for which corresponding reference data were available (see Figure 3). Parameters obtained in one stage were then carried forward unchanged to the subsequent stages. Accordingly, results shown for systems included in the optimization are denoted as fitted results, whereas calculations for data sets or solvent systems not used during parameter estimation are regarded as predictions. This distinction is important for the interpretation of the results, as it allows the quality of the fit and the transferability of the calibrated parameters to be assessed separately.

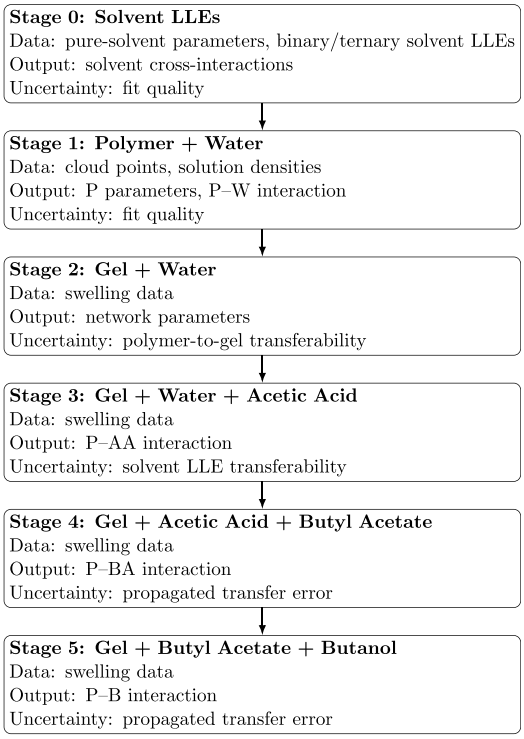

Figure 3. Sequential optimization strategy used in this work. Starting from the solvent systems, the polymer is introduced stepwise. Because data such as vapor pressure of the pure polymer are not available to fit parameters for the EOS, polymer parameters are identified only in combination with solvent data.

SOLVENT SYSTEMS

Pure-component properties of all solvents considered in this work were evaluated for each PC-SAFT parameter set and compared with experimental reference data. The resulting relative errors for liquid density and vapor pressure are summarized in Table 3.

The water parametrization of Arndt and Sadowski[30] originally proposed by Cameretti and Sadowski,[46] employs a temperature-dependent segment diameter, $\sigma(T)$, described by five adjustable parameters rather than a single constant value. This approach yields excellent agreement with experimental liquid-density data over the investigated temperature range. The parameter set of Jovein et al.[43] adopts the same water model but assumes a temperature-independent segment diameter. For the remaining components, all parameter sets generally reproduce both liquid density and vapor pressure well. Large deviations are observed for acetic acid, reflecting a well-known limitation of SAFT-based models. Acetic acid exhibits strong self-association and forms both chain-like and cyclic hydrogen-bonded structures that involve both associa-

https://doi.org/10.1021/acs.iecr.6c01731
Ind. Eng. Chem. Res. 2026, 65, 16852−16866

Table 3. Relative Errors for Pure Liquid Densities and Vapor Pressures for the Components under Consideration for Different Parameter Sets[a]

Component	Property	Arndt	Jovein	Esper	Grob
W	ρ_{liq}	0.0%	0.4%	2.4%	8.0%
	P_{LV}	0.6%	0.9%	0.6%	2.2%
B	ρ_{liq}		1.5%	0.1%	1.5%
	P_{LV}		2.1%	0.5%	2.2%
AA	ρ_{liq}		1.4%	1.4%	1.4%
	P_{LV}		2.2%	3.1%	2.2%
BA	ρ_{liq}		1.2%	0.3%	0.7%
	P_{LV}		11.6%	7.4%	2.5%

[a]DIPPR serves as reference. The DIPPR correlation was evaluated for the temperature range from 290 to 370 K. The solvents are abbreviated as water (W), butanol (B), butyl acetate (BA), and acetic acid (AA).

tion sites of a molecule, effects that are not explicitly represented by the standard SAFT association scheme.

Liquid−liquid equilibrium (LLE) predictions were subsequently evaluated for binary and ternary solvent systems. An illustrative example for the water, butyl acetate, and acetic acid system is shown in Figure 4. The nonoptimized parameter sets

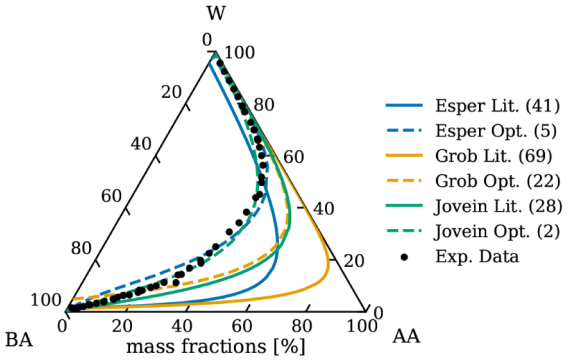

Figure 4. Ternary LLE of water (W), butyl acetate (BA), and acetic acid (AA) with calculations and experimental data.[58] All literature parameter sets (Lit.) reproduce the qualitative phase behavior but do not capture the LLE quantitatively; this agreement is improved after parameter optimization (Opt.). The model scores for this specific system are given in the legend.

exhibit pronounced deficiencies in describing the influence of acetic acid on the phase behavior. This behavior can be attributed to the lack of available binary LLE data involving acetic acid, as it is fully miscible with all other components considered. Consequently, the available binary interaction parameters are primarily fitted to vapor−liquid equilibrium data, which limits their transferability to ternary LLE predictions.

Model scores for binary and ternary systems obtained with literature and optimized parameter sets are summarized in Table 4, while Table 5 shows the fitted interaction parameters. Parameter optimization leads to a systematic improvement of the total score in phase-equilibrium predictions for all parameter sets, with the most pronounced improvements observed for ternary systems involving acetic acid. This tradeoff, in which some individual subsystems exhibit worse scores in order to improve the overall score, highlights the importance of how both the score definition and the weighting of the different systems influence the total score and final parameters. To assess whether the improvement of the ternary systems could be achieved without altering all binary interaction parameters, an additional optimization was performed in which only the acetic-acid-related k_{ij} values were adjusted. As shown in the Supporting Information, this restricted optimization did not provide a satisfactory improvement of the ternary LLE description.

POLYMER SYSTEMS

Parameterization of polymer components is inherently challenging because pure-component reference data, such as vapor pressures or liquid-state properties, are not accessible at the temperatures of interest. Consequently, polymer parameters in this work are determined exclusively from solution-phase behavior.

Following the approach of Arndt and Sadowski[30] the pNIPAM−water equilibrium was described using liquid-density data of polymer solutions in combination with liquid−liquid equilibrium (LLE) data. No experimental solubility data for pNIPAM in solvents other than water were available.

Figure 5 compiles the available experimental LLE data for pNIPAM in water; an extensive discussion is provided by Halperin et al.[59] While Halperin et al. conclude that no general consensus has been reached regarding the detailed phase behavior of pNIPAM, the reported differences of a few Kelvin in the binodal position are small relative to the temperature range considered here. A key observation across studies is the comparatively weak influence of polymer molar mass on the overall LLE envelope reported as mass fraction. This finding is particularly relevant for subsequent modeling of gel swelling, as it suggests that polymer molar mass has only a limited influence on the modeled phase behavior within the investigated range.

The Arndt and Sadowski[30] parametrization is also shown in Figure 5 for three polymer molar masses and reproduces the overall shape of the phase envelope. In these calculations,

Table 4. Model Scores for Binary and Ternary Systems Using Literature and Optimized Parameter Sets[a]

	Grob		Jovein		Esper	
System	Literature	Optimized	Literature	Optimized	Literature	Optimized
W−B	77.97	38.19	9.16	13.61	899.80	145.60
W−BA	0.50	15.31	0.45	0.58	112.09	50.69
W−B−AA	212.80	34.27	191.72	10.47	28.70	15.97
W−B−BA	30.34	2.29	1.61	3.06	5.31	45.48
W−BA−AA	69.48	21.93	27.78	1.64	40.97	5.10
Total	391.09	111.99	230.71	29.36	1086.87	262.84

[a]The score is based on the minimal geometric distance between the calculated binodals and the given solubilities from literature data.

https://doi.org/10.1021/acs.iecr.6c01731
Ind. Eng. Chem. Res. 2026, 65, 16852−16866

Table 5. Literature and Optimized Binary Interaction Parameters for the Solvent Systems Considered in This Work. Abbreviations: Water (W), Butanol (B), Butyl Acetate (BA), and Acetic Acid (AA)

	Grob		Jovein		Esper	
Pair	Literature	Optimized	Literature	Optimized	Literature	Optimized
W-B	0.03	−0.01	−0.01	−0.02	1817.48[a]	1485.36[a]
W-BA	0.11	−0.04	−0.03	−0.08	338.06[a]	−1503.82[a]
W-AA	−0.13	−0.44	−0.13	−0.71	–	3183.29[a]
B-BA	0.01	−0.02	−0.01	−0.15	1375.14[a]	447.23[a]
B-AA	−0.07	−0.61	0.12	−1.09	−0.07	−0.13
BA-AA	−0.01	−0.84	−0.14	−0.87	−0.02	−0.48

[a]Marked values correspond to ε^{AB}. All other values correspond to k_{ij}.

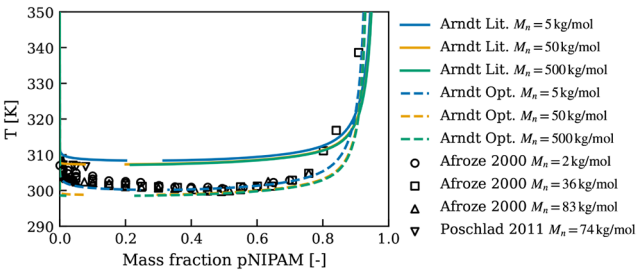

Figure 5. Experimental LLE data for pNIPAM in water at 1 atm from various sources[1,55] show only a weak dependence on polymer molar mass. Both the parametrization of Arndt et al. and an adjusted version of it reproduce this trend.

increasing molar mass shifts the critical point toward lower polymer concentrations. This behavior contrasts with that reported by Halperin et al.,[59] who argued that for pNIPAM the critical point converges to a finite, nonzero polymer mass fraction as molar mass increases, rather than continuing to shift toward the polymer-lean regime. In addition, the original Arndt and Sadowski[30] parametrization predicts a higher LCST than most of the data shown, which is consistent with its fitting primarily to the measurements of Poschlad and Enders.[39]

Using the original pNIPAM-water parameter set of Arndt and Sadowski, the experimentally observed liquid−liquid equilibrium (LLE) behavior of the polymer solution could be reproduced. The phase behavior was found to be highly sensitive to the binary interaction parameter k_{ij}. To capture the lower critical solution temperature (LCST) behavior, a temperature-dependent form of the interaction parameter was required,

$$k_{ij}(T) = k_{ij}(25^\circ\mathrm{C}) + \left(\frac{\mathrm{d}k_{ij}}{\mathrm{d}T}\right)(T - 25^\circ\mathrm{C}) \tag{12}$$

with both the intercept $k_{ij}(25\ ^\circ\mathrm{C})$ and the slope $\mathrm{d}k_{ij}/\mathrm{d}T$ at T = 25 °C serving as adjustable fitting parameters. Within the present modeling framework, the LCST behavior could not be reproduced with a temperature-independent k_{ij}.

To improve agreement with the lower LCST indicated by the compiled literature data, the intercept and slope of the temperature-dependent interaction parameter $k_{ij}(T)$ were adjusted slightly, as shown in Figure 5. The optimized values are reported in Table 6. Only minor changes in these parameters are sufficient to shift the entire phase envelope. This sensitivity is advantageous for parameter estimation, but it also implies that the thermoresponsive behavior of pNIPAM in PC-SAFT is, to a large extent, represented through the empirical temperature dependence of $k_{ij}(T)$. Accordingly, it remains an open question to what degree the LCST behavior is captured by the underlying physics of the PC-SAFT equation of state versus being effectively imposed through the chosen form of $k_{ij}(T)$.

Table 6. Summary of k_{ij} Values and the Resulting LCST for a pNIPAM and Water Solution

Parameter Set	k_{ij}	Slope k_{ij}/K^{-1}	LCST/K
Arndt Lit.	−0.175	0.002	307
Arndt Opt. ($k_{ij}(T)$)	−0.164	0.001	299

Fitting to LLE data is often ill-conditioned because large regions of the parameter space do not produce a miscibility gap or LCST behavior within the temperature and composition window of interest. In such cases, the objective function provides only limited guidance for distinguishing between poor trial parameter sets, which hampers robust optimization. To address this issue, a stepwise evaluation of parameter-set performance was introduced.

First, it was tested whether the density iterations required to calculate a given state in the NPT ensemble converged to a liquid-like root. Second, the resulting liquid densities were compared with the available experimental data.[53,54] Third, the overall LCST behavior was assessed. At this stage, it is sufficient to detect the presence of a spinodal region at the upper end of the temperature range, which can be done noniteratively and therefore at low computational cost. If an LCST-like spinodal region is identified, it is traced toward lower temperatures to obtain an estimate of the LCST. Once the calculated LCST is sufficiently close to the experimental value, the full binodal is computed and compared with the experimental solubility data.

This stepwise objective function enabled rapid and stable convergence while preserving physically consistent phase behavior. The resulting pNIPAM−water phase behavior obtained with the different water models is shown in Figure 6.

Figure 7 shows the calculated solution densities obtained with the different parametrizations; available experimental data are included for comparison. While the pNIPAM−water LLE is described over the full composition range, the density measurements cover polymer mass fractions only up to 20%. Accordingly, these data provide limited constraints at higher polymer contents.

Interpreting the calculated density in the pure-polymer limit is nontrivial. The dry polymer corresponds to a solid-like state, whereas the PC-SAFT equation of state is parametrized for the liquid phase. As a pragmatic reference, one of the few reports of the amorphous pure polymer density[60] is included in Figure 7 and used as a physically plausible benchmark. Under this interpretation, the amorphous density may serve as a

https://doi.org/10.1021/acs.iecr.6c01731
Ind. Eng. Chem. Res. 2026, 65, 16852−16866

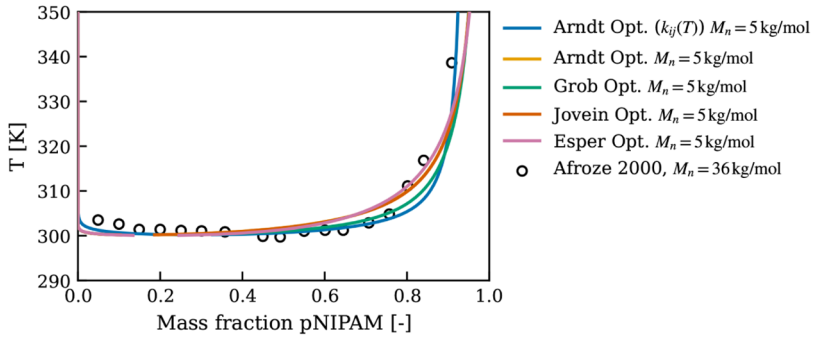

Figure 6. pNIPAM−water LLE calculated using different water parametrizations; literature data[55] are shown for comparison.

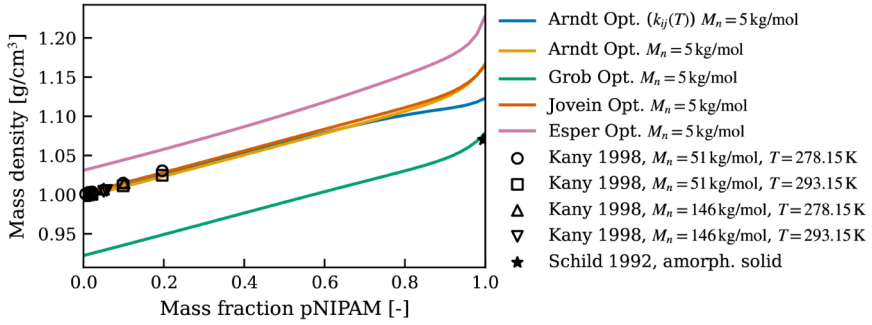

Figure 7. Solution liquid densities predicted using different water parametrizations, compared with experimental solution-density data.[53,54] The density of amorphous solid pNIPAM[60] is included as a reference for the polymer-rich limit. The calculations were performed at 293.15 K.

reasonable upper bound for densities predicted by a liquid-state EOS in the polymer-rich regime. The value has not been considered in the fitting procedure.

The experimental data indicate that the density increase between pure water and the highest measured polymer concentration is less than 3%, whereas the differences in the predicted pure-water density among the considered water parametrizations are substantially larger. Because the water model used by Arndt and Sadowski reproduces the pure-water density with high accuracy, the experimental solution densities can be used directly for that parameter set. For the remaining water models, however, the mismatch in the pure-water reference density requires an additional treatment.

Two conceptually different strategies may be considered. First, one may assume a reference value for the pure-polymer density and fit the model to excess volumes. Under this approach, a common polymer parameter set could be retained, and only the binary interaction parameters would need to be adjusted across the different water models. Second, the experimental solution densities may be shifted to match the pure-water density predicted by the respective water parametrization. However, if such a shift is applied without simultaneously revisiting the pure-polymer parameters, the resulting excess quantities may change qualitatively and thereby distort the interpretation of polymer−water interactions. Under this strategy, the polymer pure-component parameters must therefore be adjusted consistently with the shifted density data. In the present work, the second approach was adopted because the available literature data were too scarce to provide a reliable basis for specifying the pure-polymer density, despite the ambitious assumption that the density of the solid amorphous polymer can be represented by the pure-state evaluation of the EOS.

Table 7 summarizes the water parameters used in the different parameter sets. Inspection of these parameters already indicates the close similarity of the Grob, Arndt, and Jovein water models. These parametrizations exhibit stronger dispersion contributions and higher association energies compared to the Esper parameter set, together with smaller segment numbers and association volumes, that is, the complementary quantities that scale these contributions. Although all parameter sets describe pure-water properties with reasonable accuracy, a quantitatively reliable description of polymer-solution behavior requires the corresponding polymer parameters to account for these set-specific differences.

Table 7. Pure-Water Parameters[a]

Parameter set/ Source	m	σ/Å	ε/k_B	ε^{AB}/k_B	κ^{AB}
Arndt and Sadowski[30]/ Cameretti and Sadowski[46]	1.20	σ (25 °C) = 2.8	353.95	2425.67	0.045
Esper/Esper et al.[44]	2.37	2.15	230.72	2195.10	0.353
Jovein et al.[43]/ Cameretti and Sadowski[46]	1.20	2.79	353.94	2425.7	0.045
Grob and Hasse[42]/Gross and Sadowski[47]	1.07	3.00	366.51	2500.7	0.035

[a]Note that the parameter set of Jovein et al. employs a temperature-independent segment diameter and therefore does not include the temperature dependent $\sigma(T)$ formulation proposed by Cameretti and Sadowski.[46] All shown water models assume one donor site and one acceptor site as the association scheme.

https://doi.org/10.1021/acs.iecr.6c01731
Ind. Eng. Chem. Res. 2026, 65, 16852−16866

Table 8. Optimized pNIPAM Polymer Parameters for the Different Pure-Water Parameter Sets[a]

	k_{ij}	Slope k_{ij}/K^{-1}	ε_k^{AB}/k_B	κ^{AB}	ε_k/k_B	m	σ/Å
Arndt Lit.	−0.18	0.0018	175.00	0.045	297.34	60.00	5.38
Arndt Opt. ($k_{ij}(T)$)	−0.16	0.0013	175.00	0.045	297.34	60.00	5.38
Arndt Opt.	−0.28	0.0037	1341.58	0.119	224.56	60.00	5.43
Grob Opt.	−0.43	0.0029	703.20	0.119	160.36	60.00	5.58
Jovein Opt.	−0.29	0.0039	1353.31	0.120	215.87	60.00	5.42
Esper Opt.	0.01	0.0028	555.80	0.119	286.59	60.00	5.33

[a]In the case of Arndt Opt. ($k_{ij}(T)$), only the intercept and slope of the temperature-dependent binary interaction parameter $k_{ij}(T)$ were re-fitted, whereas all other polymer parameters were retained from the literature parametrization; this is also reflected in Figure 5. For the remaining cases, the full set of polymer parameters was optimized. All models used the same chain length, corresponding to a fixed molar-mass-to-m ratio, and assumed one donor−acceptor association pair per monomer unit, with each of the m segments representing a single monomer.

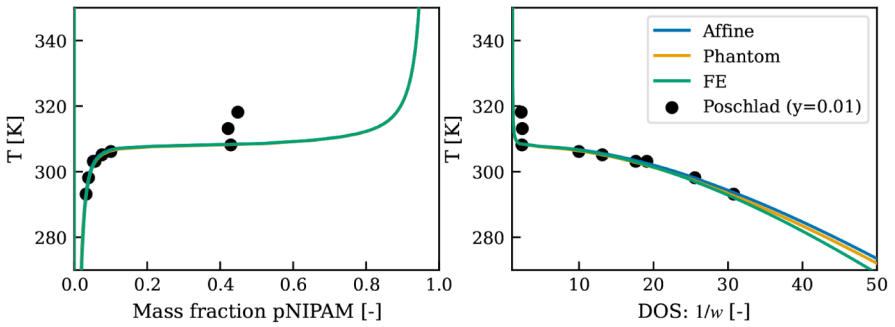

Figure 8. Effect of network-model choice on the calculated swelling behavior. The elastic contribution was evaluated using a modified network functionality. Two representations are shown: polymer mass fraction, which is closer to the pseudophase-equilibrium formulation, and degree of swelling, which is closer to the experimental representation.

Looking at Table 8, the optimized polymer parameters differ substantially between the considered parameter sets. A common feature, however, is the comparatively small association energy. This may be interpreted as a requirement to enable sufficient mixing between the polymer and water. From a simple thermodynamic perspective, long polymer chains mix only poorly with small solvent molecules because of their pronounced size asymmetry. A reduced self-association tendency of the polymer can partly counteract this effect. In particular, a small polymer association energy makes polymer−polymer association less favorable, while association with water remains favorable because of the much stronger association energy of water, if the standard mixing rules are applied in the modeling.

During the optimization, the polymer association energy had to be artificially constrained to remain positive. Because the arithmetic mean is used as the mixing rule for cross-association energies, sufficiently negative values would otherwise reduce the effective polymer−water association strength and could bias the model toward excessive mixing. At the same time, it was not possible to reproduce LCST behavior without introducing a temperature-dependent k_{ij} value. In particular, the positive slope of this temperature dependence suggests that demixing at higher temperatures is effectively imposed through the interaction parameter rather than emerging naturally from a temperature-independent interaction description. This interpretation is further supported by the preceding calculations, in which the LCST could be shifted easily by small changes in the temperature-dependent k_{ij} term.

The differences between the solvent parameter sets are not reflected in a correspondingly clear trend in the optimized polymer parameters. Several reasons may contribute to this behavior. First, even global optimization methods can struggle in high-dimensional design spaces, where pronounced local minima and broad near-optimal parameter regions can make parameter identification nonunique. Although the stochastic elements of the optimization were made reproducible by fixing the random seed, even small differences in the underlying water model can still alter the trajectory of the evolving parameter population. Second, the existence of multiple correlated parameter sets is well-known in the literature[61] and becomes more pronounced when the available data set is small and lacks physicochemical diversity.

GEL SYSTEMS

The analysis of gel systems first focuses on swelling in water, for which an extensive experimental database is available. Reported swelling degrees, however, differ between studies, reflecting the strong influence of network formation, cross-linking density, and gelation conditions on the equilibrium swelling state. These variations underline the distinction between intrinsic thermodynamic driving forces and network-specific constraints introduced during gel preparation.

Discussion of Network Theories and V_{max}

Figure 8 shows the swelling behavior of pNIPAM gels in water predicted with the parametrization of Arndt and Sadowski, together with experimental data. Two different representations are shown, as *DOS* and as polymer mass fraction w_p. As discussed in the theory section, several constitutive models are available to represent gel elasticity. In this work, three network descriptions were considered: affine, phantom, and finite extensibility (FE). While both the affine and the phantom model differ in their interpretation of the total network deformation and the dependency on the movement of network junctions, they end up in a relatively similar mathematical equation, see eq 2 and eq 3. The affine network model is often presented with a logarithmic term, which counteracts infinite

https://doi.org/10.1021/acs.iecr.6c01731
Ind. Eng. Chem. Res. 2026, 65, 16852−16866

compression. The FE model on the other hand introduces a mathematical singularity at a chosen maximal volume V_{max}, once the network approaches this volume, the elastic energy diverges as shown in eq 4.

For a consistent comparison, the elastic contribution of each model was recast in terms of a single effective network parameter, C, obtained from the corresponding idealized network interpretation based on functionality. Accordingly, the curves in Figure 8 employ C values calculated from the network functionality Φ,

$$C = \frac{\Phi - 2}{2} \tag{13}$$

as reported by Arndt and Sadowski. The network functionality shown in the plot differs from the value proposed by Arndt and Sadowski. This is due to a different integration of the elastic contribution in their approach. In the original approach, the elastic contribution appears to enter both the mechanical-equilibrium condition and the chemical-potential equilibrium. In the present work, the formulation of Maurer and Prausnitz[20] is followed, so the elastic contribution is evaluated only once, which is discussed in detail in a previous contribution.[10] As a result, the network response appears less stiff for a given network functionality. To facilitate comparison of the network contributions against the experimental data, a higher adjusted value of Φ was used. Depending on the representation, the network models are essentially indistinguishable over the investigated range.

The finite-extensibility (FE) network model is expected to become important for highly swollen gels,[19] where polymer chains are sufficiently stretched that the Gaussian-chain assumption breaks down. In the present calculations, however, incorporating FE effects does not noticeably change the predicted swelling behavior. This outcome can be rationalized by examining the underlying choice of the limiting swelling parameter, V_{max}.

Arndt and Sadowski[30] assume the fully stretched chain as the upper bound of swelling and use this state to define V_{max}, an approach that has also been adopted in the literature.[38] Under this assumption, the resulting V_{max} is very large, such that the gel remains far from the finite-extensibility regime over the swelling range considered here. As shown in the Supporting Information, the prescribed V_{max} can be estimated as

$$\frac{V_{max}}{V_{dry,collapsed}} \approx 0.94 m^2 \tag{14}$$

with the effective chain length given by

$$m_{chain} \approx m_{monomer} \frac{n_{monomer}}{n_{chain}} = m_{monomer} \frac{2}{\phi} \frac{1 - y}{y} \tag{15}$$

where y denotes the cross-linker fraction. For experimentally relevant cross-linker fractions ($y < 0.02$), this expression leads to unrealistically large values of V_{max}. Under these conditions, the finite-extensibility model essentially collapses to the affine limit. Therefore, treating V_{max} as a fitting parameter, as done by Krenn et al.[31] appears to be more physically reasonable than assuming fully stretched chains.

Considering this, all network models were separately optimized against experimental swelling data. For the finite extensibility model, two approaches were investigated. In the first, the maximum swelling volume V_{max} was fixed based on the tetrahedral limit of fully stretched network chains. In the second approach, a factor for V_{max} was treated as an adjustable parameter, describing the assumed V_{max} in comparison to the V_{max} in the fully stretched limit. As summarized in Table 9, the finite-extensibility (FE) model with a predetermined V_{max} is effectively indistinguishable from the affine network model when fitted to a single experimental data set, since the optimization leaves the scaling factor of V_{max} unchanged. All models extrapolate the qualitative trend to the second data set correctly, but substantial quantitative deviations remain. When both data sets are fitted simultaneously, the resulting parameters reflect a compromise between the two fit qualities. In principle, the FE model with an adjustable scaling factor could provide an advantage because the resulting V_{max} depends on the cross-linker content y. In practice, the overall improvement remains negligible. The present results indicate that a single-parameter network description is sufficient for the systems considered. The original parameters show a higher score as the integration of the network resulted in a stiffer response.

Table 9. Parameters and Scores for Different Polymer Network Models[a]

Network model	Φ	ϕ_{ref}	Factor V_{max}	Score (y = 0.01)	Score (y = 0.015)
Original publication					
Affine	2.24	1.0	-	1.51	2.46
Phantom	2.24	1.0	-	1.42	2.31
FE	2.24	1.0	100%	1.35	2.10
Optimized for y = 0.01					
Affine	2.69	1.0	-	0.06	0.40
Phantom	2.66	1.0	-	0.05	0.31
FE	2.66	1.0	100%	0.06	0.34
FE (adjusted V_{max})	2.66	1.0	77%	0.06	0.32
Optimized on both (y = 0.01 and y = 0.015)					
Affine	2.89	1.0	-	0.14	0.18
Phantom	2.82	1.0	-	0.16	0.15
FE	2.77	1.0	100%	0.10	0.22
FE (adjusted V_{max})	2.76	1.0	46%	0.12	0.19

[a]The original parameters show a higher score as the integration of the network resulted in a stiffer response. The score is defined as the average relative errors, where higher values indicate poorer performance, see eq 11.

Extrapolative Estimation of Network Stiffness and Length of Chains

The previous results highlighted the extrapolative capability of all network models over a range of cross-linking contents. The intuitive expectation that increasing cross-link density results in a stiffer network is inherently captured by network theories, albeit not always in a transparent manner. The parameter C provides the most direct measure of network stiffness. Although C may be linked to idealized network characteristics such as the functionality Φ, it is typically handled as an adjustable parameter in practical applications. Notably, even for identical network functionality, and therefore identical C, the predicted mechanical response becomes increasingly stiff with higher cross-linking content y.

A further, less apparent but equally important factor influencing the elastic behavior is the polymer chain length, or molar mass, assumed in the network representation. This is

https://doi.org/10.1021/acs.iecr.6c01731
Ind. Eng. Chem. Res. 2026, 65, 16852−16866

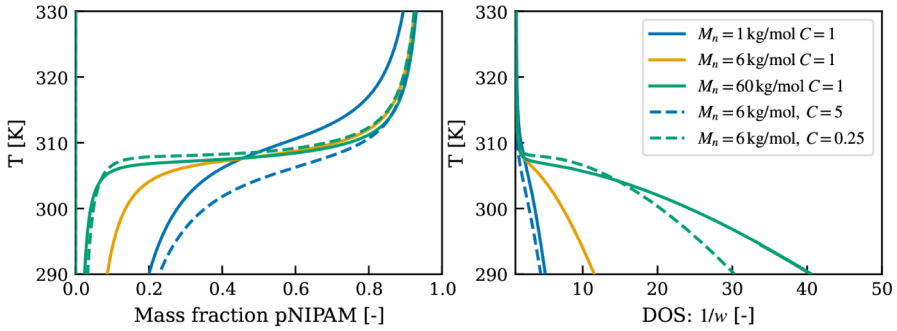

Figure 9. Both the choice of the effective chain length and the stiffness parameter C directly affect the predicted gel stiffness.

illustrated in Figure 9, which shows that both the molar mass M_n and the elastic factor C influence the magnitude of the predicted swelling response. While the polymer systems showed that molar mass has only a limited effect on the polymer−solvent liquid−liquid equilibrium, it can substantially alter the swelling behavior. This contrast indicates that molar mass is of minor importance for solution phase boundaries within the investigated range, but may become a dominant factor in gel swelling because of its role in governing network elasticity.

At first glance, this appears counterintuitive because a cross-linked gel does not have a uniquely defined molar mass in the same sense as a linear polymer. However, inspection of the derivation of the elastic contribution following the affine or the phantom network approach clarifies the origin of this dependence. In both cases, the network elasticity is built from the free energy of an ideal Gaussian chain. The macroscopic elastic free energy is then obtained by summing over the contributions of all network strands; equivalently, the elastic contribution scales approximately linearly with the number of elastically active chains. Consequently, assumptions about an effective chain length, or strand molar mass between cross-links, directly affect the predicted stiffness and, hence, the swelling degree. Figure 10 illustrates this concept schematically using multiple ideal Gaussian chains that follow random-walk statistics on a lattice.

Using the ensemble average of the root mean squared end-to-end vector, i.e., the vector connecting the first and last segment of a polymer chain, it can be shown[62] that the characteristic end-to-end distance scales as $\sqrt{N}$, where N is the number of segments per chain. Following the notation of Mark and Erman[24] the elastic free energy of a single ideal Gaussian chain can be written as

$$A^{\mathrm{el}} = A^{*}(T) + \frac{3}{2}kT\frac{r^2}{\langle r^2\rangle_0} \tag{16}$$

where r is the end-to-end distance and $\langle r^2\rangle_0$ is the mean-squared end-to-end distance in the reference state. Subtracting the reference state and summing over all n_{chain} elastically active chains yields

$$\Delta A^{\mathrm{el}} = n_{\mathrm{chain}}\frac{3}{2}kT\left(\frac{\langle r^2\rangle}{\langle r^2\rangle_0} - 1\right) \tag{17}$$

which serves as the common starting point for the affine, phantom, and FE network models.

This expression also clarifies why the assumed chain length influences the predicted swelling. The reference size $\langle r^2\rangle_0$ does not decrease linearly with decreasing chain length, whereas the assumed number of chains n_{chain} in a fixed polymer mass is bound to increase proportionally as the assumed chain length decreases. As a result, the total elastic contribution increases for shorter assumed chains and the modeled gel response becomes stiffer.

This sensitivity is important when selecting an effective chain length for the network model and may motivate a more rigorous estimate than simply adopting an average strand length between junctions. It should also be kept in mind that the Gaussian-chain derivation formally assumes sufficiently long chains; depending on the chosen chain length, the number of segments may become too small for the Gaussian approximation to be justified. This is where the FE network can compensate and offer an improved extrapolative capability for different cross-linking contents. Although Table 9 provides only limited justification for using this model for a single data set, a more physically grounded estimate of V_{max} as a function of chain length or cross-linking content may still help tailor the network response to a given cross-linking procedure.

The chain length used in the elasticity model does not necessarily have to coincide with that used in the thermodynamic model. For the present polymer system, the chain length has no significant influence on the pNIPAM−water LLE behavior, which provides the practical advantage that a single chain length can be used consistently in both the thermodynamic and elastic descriptions. For gels cross-linked during polymerization, the strand length may be estimated using eq 15. For physically cross-linked networks (e.g., freeze−

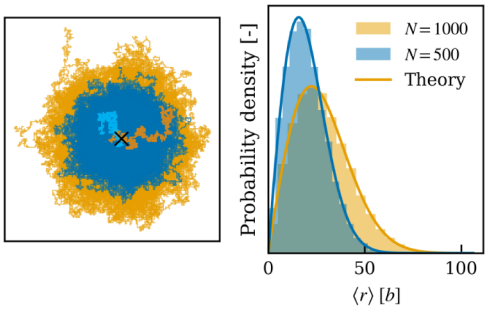

Figure 10. Schematic representation of ideal Gaussian chains with varying segment numbers, N, obtained from 5×10^4 random walks. The trajectories on the left and their corresponding end-to-end distance distributions on the right show that the characteristic size of the chains increases with chain length. Since the elasticity of polymer networks is determined by the free-energy contributions of these chains, the choice of effective chain length directly influences the predicted stiffness and swelling behavior of the gel.

https://doi.org/10.1021/acs.iecr.6c01731
Ind. Eng. Chem. Res. 2026, 65, 16852−16866

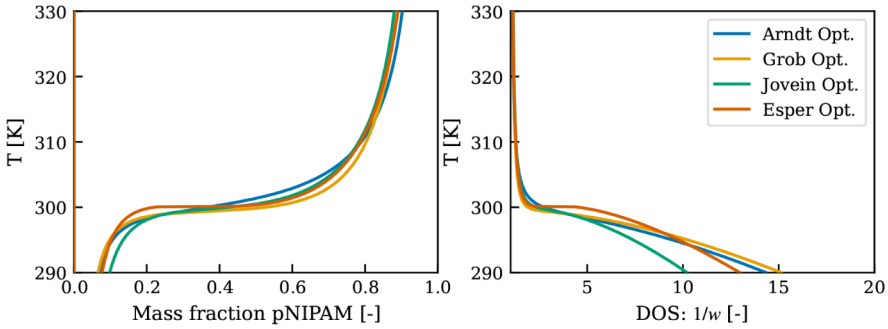

Figure 11. Calculated swelling behavior obtained with different polymer−water parametrizations while keeping the network parameters fixed. The spread in the predicted gel-swelling curves is of similar magnitude to the differences between the underlying polymer-solution binodals.

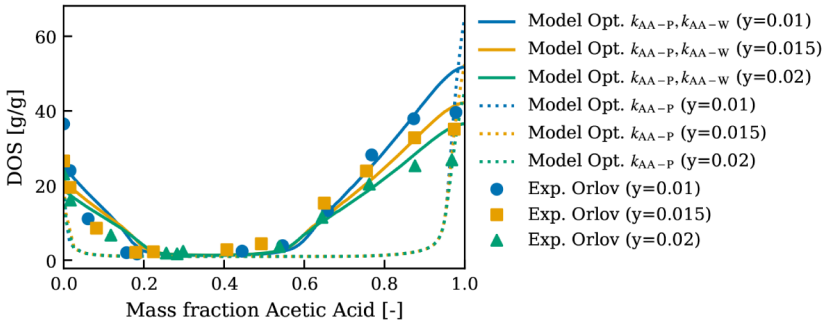

Figure 12. Calculated degree of swelling in the ternary system pNIPAM-water-acetic acid for two optimization strategies. Optimization of k_{AA-P} alone predicts an excessively strong cononsolvency effect, whereas simultaneous optimization of k_{AA-P} and k_{AA-W} yields improved agreement with the experimental data of Orlov et al.[57] The parameters were optimized for a cross-linking content of y = 0.015; all other curves are predictions.

thawing), alternative estimation strategies may be required. Nevertheless, applying the same network-model framework remains feasible, provided that the chosen effective chain length is interpreted accordingly.

Transferability of Network Parameters to Different Water Parametrizations

Figure 11 illustrates the effect of using different water parametrizations while keeping the network parameters fixed. The spread between the predicted gel swelling curves is of the same order as the differences between the underlying polymer-solution binodals.

This comparison highlights the transferability of the network description. Although different polymer−water parametrizations are employed to represent the same experimental binodal, using identical network parameters yields very similar swelling predictions. This observation supports a contribution-wise interpretation of gel behavior: the equation of state primarily determines the thermodynamic driving force through the polymer-solution phase behavior, whereas the network model sets the elastic resistance and thus the swelling magnitude. Within the investigated range, these contributions appear to be comparatively decoupled, which suggests that calibrated network parameters may be transferred when changing the solvent parametrization. This, in turn, motivates applying the same network parameters to swelling predictions in organic solvents.

Optimization for Organic Solvents

For industrial applications, hydrogels are commonly exposed to a range of solvent environments. A reliable description of swelling in mixed solvents is therefore essential. As discussed in the methodology section, however, experimental swelling data for such systems are scarce. In this work, ternary gel systems along the sequence water and acetic acid, acetic acid and butyl acetate, butyl acetate and butanol are considered. This chain-like transfer of information introduces a significant risk of error propagation. In addition, the binary solvent-solvent interactions are themselves estimated from binary and ternary liquid−liquid equilibrium (LLE) data.

Figure 12 shows the calculated swelling behavior of the gel in water-acetic acid mixtures. The experimental data of Orlov et al.[57] exhibit cononsolvency, a phenomenon also reported for water−alcohol mixtures.[63] In the present modeling approach, the polymer-acetic acid interaction is the only unknown parameter, whereas the solvent-solvent interaction is taken from the preceding solvent-system optimization. With this parameter set, the model predicts a pronounced cononsolvency effect but overestimates its strength relative to experiment. Simultaneous optimization of k_{AA-P} and k_{AA-W} yields substantially better agreement, illustrating the sensitivity of the prediction to the transferred solvent interaction parameter.

This result highlights a central limitation of the transfer strategy. The interaction between water and acetic acid cannot be constrained directly from LLE at the conditions of interest, since the mixture does not exhibit a miscibility gap in this range. Its interaction parameter must therefore be inferred indirectly, for example from other phase-equilibrium data obtained under different conditions. The problem is further complicated by the association behavior of acetic acid and by the general difficulty of accurately representing water. The present results therefore underscore the extent to which parameter fitting remains unavoidable in this class of models.

At the same time, the fitted parameters retain a plausible physical interpretation. As shown in Table 10, the water-acetic acid interaction parameter is strongly negative, indicating a strong mutual attraction. This favors preferential water-acetic

https://doi.org/10.1021/acs.iecr.6c01731
Ind. Eng. Chem. Res. 2026, 65, 16852−16866

Table 10. Fitted Binary Interaction Parameters k_{ij} for the Ternary System pNIPAM-Water-Acetic Acid. Unless Stated Otherwise, the Value of k_{AA-W} was Taken from the Preceding Solvent-System Optimization

Optimized parameters	k_{AA-P}	k_{AA-W}
k_{AA-P}, k_{AA-W}	−0.067	−0.267
k_{AA-P}	−0.146	*−0.707*

acid interactions in the mixed solvent and provides a plausible explanation for the calculated cononsolvency, consistent with mechanistic interpretations discussed in the literature.[63] The more negative value of k_{AA-W} obtained from solvent-system optimization therefore explains the stronger cononsolvency predicted in that case.

The effect of cross-linking is captured reasonably well, particularly given that the parameters were optimized only for y = 0.015. The remaining data sets therefore represent genuine predictions. A fourth data set reported by Orlov et al.[57] concerning the influence of the polymerizable fraction during gel synthesis is not shown here. In principle, this effect should also be representable within the model through an appropriate choice of ϕ_{ref}.

Figure 13 shows the ternary pNIPAM-acetic acid-butyl acetate system, with Table 11 showing the values of the optimized parameters. For pure acetic acid and a cross-linking content of y = 0.01, the data reported by Orlov et al.[57] indicate a degree of swelling of approximately $DOS \approx 40$, whereas the data of Eckert et al.[4] give a value of only $DOS \approx 20$ for the same cross-linking content. This substantial difference illustrates a general difficulty in the interpretation of gel swelling experiments.

The swelling model employed here relies on simplified assumptions. In particular, effects related to the actual network topology, the gel preparation process, and the choice of reference volume are not represented explicitly; the network functionality serves as the only descriptor of the topology. The data demonstrate that quantitative swelling values must be interpreted with care. From the perspective of the underlying thermodynamics, however, the difference in swelling is comparatively small. Within the pseudophase approximation, the corresponding polymer mass fractions in the gel phase are approximately w = 1/40 = 2.5% and w = 1/20 = 5%, respectively, which represents only a minor absolute difference. Thus, while the change in DOS appears dramatic experimentally, its impact on the thermodynamic description is less pronounced and is to a large extent associated with the assumed elastic contribution.

Table 11. Fitted Binary Interaction Parameters k_{ij} and Network Functionality Φ for the Ternary System pNIPAM-Acetic Acid-Butyl Acetate[a]

Optimized parameters	Φ	k_{P-BA}	k_{AA-BA}
k_{P-BA}	*2.694*	1.892	*−0.700*
Φ	4.691	*0.000*	*−0.700*
Φ, k_{P-BA}	4.534	0.049	*−0.700*
Φ, k_{P-BA}, k_{AA-BA}	4.542	0.001	−0.045

[a]Italic values were not optimized for the given data set.

Nevertheless, Figure 13 shows that adjusting only the polymer-butyl acetate interaction parameter k_{BA-P} leads to poor agreement with the experimental data. Although the strong deswelling induced by butyl acetate is captured qualitatively, the optimization fails to provide a satisfactory quantitative description. To reproduce the swelling in pure acetic acid, either the interaction parameter k_{AA-P} or the network functionality Φ would need to be adjusted. Following the previous discussion, modifying k_{AA-P} would alter the underlying thermodynamic behavior of the polymer system and would therefore conflict with the preceding calculations. Adjusting the network functionality appears more reasonable, since variations in network topology may arise from the preparation process. When this adjustment is combined with a modification of the solvent-solvent interaction parameter k_{AA-BA}, good agreement with the experimental data can be obtained.

Figure 14 shows the continuation of the fitting procedure for the ternary pNIPAM-butyl acetate-butanol system, with Table 12 showing the values of the optimized parameters. In this case, the experimental data originate from the same source[4] and were obtained under the same process conditions, so that the same network parameters can reasonably be assumed. Starting from the collapsed state in pure butyl acetate, the swelling in butanol can be described qualitatively. However, as in the previous system, fitting only the polymer-butanol interaction parameter k_{P-B} yields comparatively poor results, whereas allowing the solvent-solvent interaction parameter k_{BA-B} to be adjusted improves the agreement. This improvement, however, comes at the cost of introducing an additional fitted binary interaction parameter, which differs in both sign and magnitude from the value obtained from the solvent-system optimization.

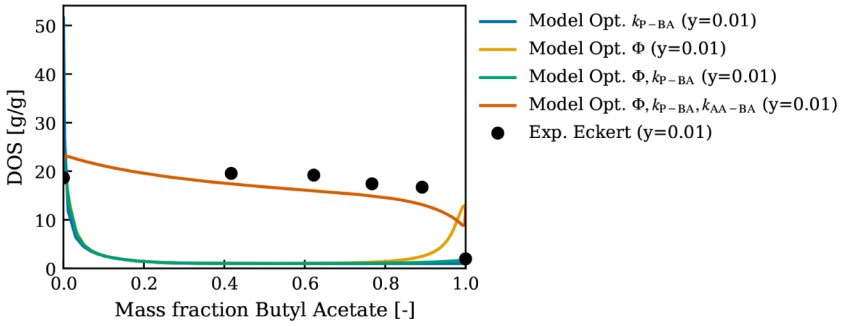

Figure 13. Calculated degrees of swelling in the ternary pNIPAM-acetic acid-butyl acetate system for different optimization strategies. Optimization of only the single parameter k_{BA-P}, in accordance with the described methodology, yields poor agreement with the experimental data. Since the swelling degrees in pure acetic acid reported by Orlov et al.[57] and Eckert et al.[4] differ significantly, the network functionality was additionally adjusted.

https://doi.org/10.1021/acs.iecr.6c01731
Ind. Eng. Chem. Res. 2026, 65, 16852−16866

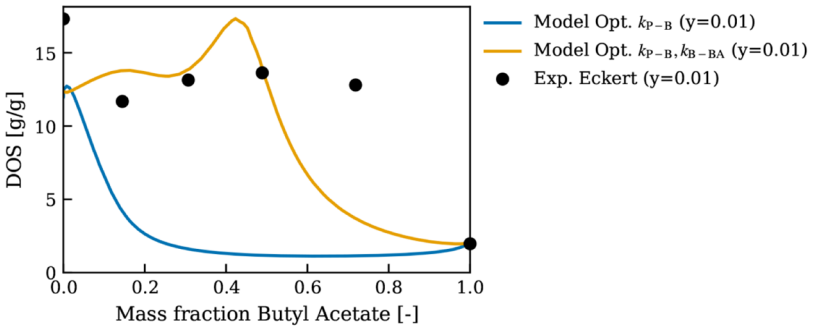

Figure 14. Calculated degrees of swelling in the ternary pNIPAM-butyl acetate-butanol system for different optimization strategies. Optimization of only the single parameter k_{B-P}, in accordance with the described methodology, yields poor agreement with the experimental data.

Table 12. Fitted Binary Interaction Parameters k_{ij} for the Ternary System pNIPAM-Butyl Acetate-Butanol[a]

Optimized parameters	k_{P-B}	k_{B-BA}
k_{P-B}	0.028	*-0.148*
k_{P-B}, k_{B-BA}	0.029	0.029

[a]Italic values were not optimized for the given data set.

Overall, these results highlight the limited transferability of binary interaction parameters. Since these parameters lack a fully independent physical basis, especially in the context of the remaining model parameters, they effectively compensate for missing physics in the specific system for which they were fitted. Their transfer to other systems may still preserve qualitative trends, such as whether certain components interact more attractively, negative k_{ij}, or more repulsively, positive k_{ij}. However, the quantitative magnitude, scaling behavior, and extension to multicomponent mixtures do not necessarily extrapolate well. In the present work, the interaction parameters therefore had to be adjusted for the specific ternary systems considered.

This suggests that future parameter estimation may benefit from a global optimization strategy in which the full set of parameters is fitted simultaneously to a comprehensive set of data, rather than stepwise for individual subsystems. In this context, Walker et al.[61] reported strong correlations among pure-component parameters, indicating that a parametrization based solely on pure-component properties may not always represent the underlying physics adequately. A multicomponent objective function may therefore provide a more robust route for future parametrizations, such that contribution-based parameter estimation is more closely linked to the physicochemical properties of the respective components.

CONCLUSION

In this work, a consistent PC-SAFT-based framework for gel-equilibrium calculations in multicomponent solvent systems was established and applied to stimuli-responsive gels relevant to smart materials and smart reactor concepts. The solvent system was parametrized step by step, solvent thermodynamics were coupled with gel elasticity, and swelling behavior in complex mixtures was analyzed using the resulting model. In this way, both the practical strength of the framework and its central limitation were demonstrated: good agreement with experiment can be achieved, but not with a unique or physically unambiguous parameter set.

A strong dependency chain within the parametrization was identified as a key result. Acetic acid could not be fitted directly from binary liquid−liquid equilibrium data and therefore had to be identified through ternary systems, while the polymer parameters had to be obtained from solution data rather than from a pure-component reference state. It was shown that fitted parameters do not simply reflect isolated component properties, but that compensation effects from the overall fitting strategy are also absorbed. It was therefore made clear that robustness, identifiability, and transferability are just as important as fit quality, and that the physical interpretability of the model is likely to be improved by a broader experimental basis with chemically diverse solvents.

Beyond parameter estimation, key conceptual aspects of EOS-based gel modeling were also clarified, including the role of the elastic contribution and the implications of the pseudophase approximation. By comparing different network models, it was further shown that additional model complexity does not automatically lead to better predictions.

Overall, a transparent and practically useful tool for describing responsive gels in complex solvent environments is provided by this work in combination with PC-SAFT. It is shown which aspects can already be modeled reliably, where the current limits lie, and which data and assumptions are most important for future predictive applications.

ASSOCIATED CONTENT

Data Availability Statement

The data and source code required to fully reproduce the figures presented in this paper are publicly available at 10.15480/882.16926.

Supporting Information

The Supporting Information is available free of charge at https://pubs.acs.org/doi/10.1021/acs.iecr.6c01731.

Additional numerical details and the nomenclature are provided in the Supporting Information (PDF)

AUTHOR INFORMATION

Corresponding Authors

Nanning Jaeschke − *Institute of Thermal Separation Processes, Hamburg University of Technology, Hamburg 21073, Germany;* orcid.org/0009-0000-0369-3568; Email: nanning.jaeschke@tuhh.de

Walter G. Chapman − *Department of Chemical and Biomolecular Engineering, Rice University, Houston, Texas 77005-1827, United States;* orcid.org/0000-0002-8789-9041; Email: wgchap@rice.edu

https://doi.org/10.1021/acs.iecr.6c01731
Ind. Eng. Chem. Res. 2026, 65, 16852−16866

Author

Irina Smirnova − *Institute of Thermal Separation Processes, Hamburg University of Technology, Hamburg 21073, Germany;* orcid.org/0000-0003-4503-4039

Complete contact information is available at: https://pubs.acs.org/10.1021/acs.iecr.6c01731

Notes

The authors declare no competing financial interest.

■ ACKNOWLEDGMENTS

The authors gratefully acknowledge the use of Avogadro 2[64] to construct and visualize the NIPAAm molecular structure shown in the graphical abstract. The FeOs package[65] was used to perform the thermodynamic calculations, and the authors thank its developers for providing clear, comprehensive, and well-structured documentation. This project is funded by the Deutsche Forschungsgemeinschaft (DFG, German Research Foundation) − SFB 1615 − 503850735.

■ REFERENCES

(1) Poschlad, K.; Enders, S. Thermodynamics of aqueous solutions containing poly (N-isopropylacrylamide). *J. Chem. Thermodyn.* **2011**, *43*, 262−269.

(2) Althans, D.; Langenbach, K.; Enders, S. Influence of different alcohols on the swelling behaviour of hydrogels. *Mol. Phys.* **2012**, *110*, 1391−1402.

(3) Zhi, D.; Huang, Y.; Han, X.; Liu, H.; Hu, Y. A molecular thermodynamic model for temperature- and solvent-sensitive hydrogels, application to the swelling behavior of PNIPAm hydrogels in ethanol/water mixtures. *Chem. Eng. Sci.* **2010**, *65*, 3223−3230.

(4) Eckert, K. M.; Müller, S.; Luinstra, G. A.; Smirnova, I. Exploring pNIPAM lyogels: Experimental study on swelling equilibria in various organic solvents and mixtures, supported by COSMO-RS analysis. *Fluid Phase Equilib.* **2024**, *586*, 114182.

(5) Eckert, K. M.; Bonsen, J.; Hajnal, A.; Gmeiner, J.; Hasse, J.; Adrian, M.; Karsten, J.; Kißling, P. A.; Penn, A.; Fiedler, B.; Luinstra, G. A.; Smirnova, I. Enhancing swelling kinetics of pNIPAM lyogels: The role of crosslinking, copolymerization, and solvent. *Fluid Phase Equilib.* **2025**, *597*, 114462.

(6) Singh, J.; Nayak, P. pH-responsive polymers for drug delivery: Trends and opportunities. *J. Polym. Sci.* **2023**, *61*, 2828−2850.

(7) Gandhi, A.; Paul, A.; Sen, S. O.; Sen, K. K. Studies on thermoresponsive polymers: Phase behaviour, drug delivery and biomedical applications. *Asian J. Pharm. Sci.* **2015**, *10*, 99−107.

(8) Döring, A.; Birnbaum, W.; Kuckling, D. Responsive hydrogels − structurally and dimensionally optimized smart frameworks for applications in catalysis, micro-system technology and material science. *Chem. Soc. Rev.* **2013**, *42*, 7391.

(9) Hu, X.; Spille, C.; Schlüter, M.; Smirnova, I. Smart Structures−Additive Manufacturing of Stimuli-Responsive Hydrogels for Adaptive Packings. *Ind. Eng. Chem. Res.* **2020**, *59*, 19458−19464.

(10) Jaeschke, N.; Chapman, W. G.; Smirnova, I. Lyogel Equilibria with Helmholtz Equations of State. Part I: A Robust Second-Order Framework. *Ind. Eng. Chem. Res.* **2026**, DOI: 10.1021/acs.iecr.6c01490.

(11) Lindvig, T.; Michelsen, M. L.; Kontogeorgis, G. M. Liquid-Liquid Equilibria for Binary and Ternary Polymer Solutions with PC-SAFT. *Ind. Eng. Chem. Res.* **2004**, *43*, 1125−1132.

(12) Von Solms, N.; Kouskoumvekaki, I. A.; Lindvig, T.; Michelsen, M. L.; Kontogeorgis, G. M. A novel approach to liquid-liquid equilibrium in polymer systems with application to simplified PC-SAFT. *Fluid Phase Equilib.* **2004**, *222−223*, 87−93.

(13) Michelsen, M. L.; Mollerup, J. M. *Thermodynamic models: Fundamentals & computational aspects*; Tie-Line Publications: Holte, 2007.

(14) Chapman, W.; Gubbins, K.; Jackson, G.; Radosz, M. SAFT: Equation-of-state solution model for associating fluids. *Fluid Phase Equilib.* **1989**, *52*, 31−38.

(15) Gross, J.; Sadowski, G. Perturbed-Chain SAFT: An Equation of State Based on a Perturbation Theory for Chain Molecules. *Ind. Eng. Chem. Res.* **2001**, *40*, 1244−1260.

(16) Jaeschke, N.; Smirnova, I.; Chapman, W. G. Lyogel Equilibria with Helmholtz Equations of State: Source Code, Data repository, 2026. https://doi.org/10.15480/882.16926.

(17) Flory, P. J.; Rehner, J. Statistical Mechanics of Cross-Linked Polymer Networks II. Swelling. *J. Chem. Phys.* **1943**, *11*, 521−526.

(18) James, H. M.; Guth, E. Theory of the Elastic Properties of Rubber. *J. Chem. Phys.* **1943**, *11*, 455−481.

(19) Miao, B.; Vilgis, T. A.; Poggendorf, S.; Sadowski, G. Effect of Finite Extensibility on the Equilibrium Chain Size. *Macromol. Theory Simul.* **2010**, *19*, 414−420.

(20) Maurer, G.; Prausnitz, J. Thermodynamics of phase equilibrium for systems containing gels. *Fluid Phase Equilib.* **1996**, *115*, 113−133.

(21) Escobedo, F. A.; De Pablo, J. J. Molecular simulation of polymeric networks and gels: phase behavior and swelling. *Phys. Rep.* **1999**, *318*, 85−112.

(22) Hild, G. Interpretation of equilibrium swelling data on model networks using affine and 'phantom' network models. *Polymer* **1997**, *38*, 3279−3293.

(23) Cicalese, M.; Gloria, A.; Ruf, M. In From Statistical Polymer Physics to Nonlinear Elasticity. *Archive For Rational Mechanics And Analysis*; Springer, 2020; Vol. *236*, pp 1127−1215.

(24) Mark, J. E.; Erman, B. *Rubberlike elasticity: A molecular primer*; Cambridge University Press, 2007.

(25) Flory, P. J.; Rehner, J. Statistical Mechanics of Cross-Linked Polymer Networks I. Rubberlike Elasticity. *J. Chem. Phys.* **1943**, *11*, 512−520.

(26) Flory, P. J. *Principles of Polymer Chemistry*; Cornell University Press, 1953.

(27) James, H. M.; Guth, E. Theory of the Increase in Rigidity of Rubber during Cure. *J. Chem. Phys.* **1947**, *15*, 669−683.

(28) James, H. M.; Guth, E. Simple presentation of network theory of rubber, with a discussion of other theories. *J. Polym. Sci.* **1949**, *4*, 153−182.

(29) James, H. M.; Guth, E. Statistical Thermodynamics of Rubber Elasticity. *J. Chem. Phys.* **1953**, *21*, 1039−1049.

(30) Arndt, M. C.; Sadowski, G. Modeling Poly(*N* -isopropylacrylamide) Hydrogels in Water/Alcohol Mixtures with PC-SAFT. *Macromolecules* **2012**, *45*, 6686−6696.

(31) Krenn, P.; Zimmermann, P.; Fischlschweiger, M.; Zeiner, T. Modeling Highly Cross-Linked Epoxy Resins in Solvents of Different Polarities with PC-SAFT. *Ind. Eng. Chem. Res.* **2020**, *59*, 5133−5141.

(32) Hüther, A.; Xu, X.; Maurer, G. Swelling of n-isopropyl acrylamide hydrogels in water and aqueous solutions of ethanol and acetone. *Fluid Phase Equilib.* **2004**, *219*, 231−244.

(33) Flory, P. J. Thermodynamic relations for high elastic materials. *Trans. Faraday Soc.* **1961**, *57*, 829.

(34) Wall, F. T.; Flory, P. J. Statistical Thermodynamics of Rubber Elasticity. *J. Chem. Phys.* **1951**, *19*, 1435−1439.

(35) Flory, P. J. Theory of elasticity of polymer networks. The effect of local constraints on junctions. *J. Chem. Phys.* **1977**, *66*, 5720−5729.

(36) Flory, P. J.; Gordon, M.; McCrum, N. G. Statistical Thermodynamics of Random Networks. *Proc. R. Soc. London, Ser. A* **1976**, *351*, 351−380.

(37) Hüther, A.; Maurer, G. Swelling of *N*-isopropyl acrylamide hydrogels in aqueous solutions of poly(ethylene glycol). *Fluid Phase Equilib.* **2004**, *226*, 321−332.

(38) Liu, J.; Chapman, W. G. Thermodynamic Modeling of the Equilibrium Partitioning of Hydrocarbons in Nanoporous Kerogen Particles. *Energy Fuels* **2019**, *33*, 891−904.

(39) Poschlad, K.; Enders, S. Thermodynamics of aqueous solutions containing poly (N-isopropylacrylamide) and vitamin C. *Fluid Phase Equilib.* **2011**, *302*, 153−160.

(40) Arndt, M. C. *Thermodynamic modelling of hydrogels*, Ph.D. thesis; TU Dortmund, 2014.
(41) Wagner, S.; Nagl, R.; Weissensteiner, A.; Strunčnik, J.; Schönbacher, L.; Gschwandl, M.; Fischlschweiger, M.; Zeiner, T. Solvent Diffusion Modeling in Silicone. *J. Chem. Eng. Data* **2024**, *69*, 472−481.
(42) Grob, S.; Hasse, H. Thermodynamics of Phase and Chemical Equilibrium in a Strongly Nonideal Esterification System. *J. Chem. Eng. Data* **2005**, *50*, 92−101.
(43) Jovein, I. B.; Baco, S.; Sadowski, G.; Doghieri, F.; Giacinti Baschetti, M.; Yu, G.; Leveneur, S.; Legros, J.; Held, C. Comprehensive Compilation on Esterification Reactions and Predicting Reaction Kinetics and Equilibrium Using PC-SAFT. *ACS Engineering Au* **2025**, *5*, 234−246.
(44) Esper, T.; Bauer, G.; Rehner, P.; Gross, J. PCP-SAFT Parameters of Pure Substances Using Large Experimental Databases. *Ind. Eng. Chem. Res.* **2023**, *62*, 15300−15310.
(45) Rehner, P.; Bardow, A.; Gross, J. Modeling Mixtures with PCP-SAFT: Insights from Large-Scale Parametrization and Group-Contribution Method for Binary Interaction Parameters. *Int. J. Thermophys.* **2023**, *44* (12), 179.
(46) Cameretti, L. F.; Sadowski, G. Modeling of aqueous amino acid and polypeptide solutions with PC-SAFT. *Chem. Eng. Process.* **2008**, *47*, 1018−1025.
(47) Gross, J.; Sadowski, G. Application of the Perturbed-Chain SAFT Equation of State to Associating Systems. *Ind. Eng. Chem. Res.* **2002**, *41*, 5510−5515.
(48) Moine, E.; Piña-Martinez, A.; Jaubert, J.-N.; Sirjean, B.; Privat, R. I-PC-SAFT: An Industrialized Version of the Volume-Translated PC-SAFT Equation of State for Pure Components, Resulting from Experience Acquired All through the Years on the Parameterization of SAFT-Type and Cubic Models. *Ind. Eng. Chem. Res.* **2019**, *58*, 20815−20827.
(49) American Institute of Chemical Engineers. *DIPPR 801 Database*; 2025. https://www.aiche.org/dippr/projects/801.
(50) Gomis, V.; Font, A.; Saquete, M. D.; García-Cano, J. Isothermal (liquid + liquid) equilibrium data at T = 313.15 K and isobaric (vapor + liquid + liquid) equilibrium data at 101.3 kPa for the ternary system (water + 1-butanol + p-xylene). *J. Chem. Thermodyn.* **2014**, *79*, 242−247.
(51) Smirnov, A.; Sadaeva, A.; Podryadova, K.; Toikka, M. Quaternary liquid-liquid equilibrium, solubility and critical states: Acetic acid − n-butanol − n-butyl acetate − water at 318.15 K and atmospheric pressure. *Fluid Phase Equilib.* **2019**, *493*, 102−108.
(52) Stephenson, R.; Stuart, J. Mutual binary solubilities: water-alcohols and water-esters. *J. Chem. Eng. Data* **1986**, *31*, 56−70.
(53) Kany, H. P. *Thermodynamische Eigenschaften wäßriger Polymer-Lösungen*; Shaker: Aachen, 1998.
(54) Wohlfarth, C. *CRC handbook of thermodynamic data of aqueous polymer solutions*; CRC Press: Boca Raton, 2004.
(55) Afroze, F.; Nies, E.; Berghmans, H. Phase transitions in the system poly(N-isopropylacrylamide)/water and swelling behaviour of the corresponding networks. *J. Mol. Struct.* **2000**, *554*, 55−68.
(56) Poschlad, K. *Experimentelle und theoretische Untersuchungen der Wirkstoffaufnahme und -abgabe von Poly-(N-isopropylacrylamid)-Hydrogelen*. Ph.D. thesis; TU Berlin, 2011.
(57) Orlov, Y.; Xu, X.; Maurer, G. Swelling of nonionic N-isopropyl acrylamide hydrogels in aqueous solutions of (acetic acid or pyridine). *Fluid Phase Equilib.* **2005**, *238*, 87−94.
(58) Bevia, F. R.; Rico, D. P.; Yagües, V. G.; Galvan, P. V. Quaternary liquid-liquid equilibrium: water-acetic acid-1-butanol-n-butyl acetate at 25°C. *Fluid Phase Equilib.* **1984**, *18*, 171−183.
(59) Halperin, A.; Kröger, M.; Winnik, F. M. Poly(N − isopropylacrylamide) Phase Diagrams: Fifty Years of Research. *Angew. Chem. Int. Ed.* **2015**, *54*, 15342−15367.
(60) Schild, H. Poly(N-isopropylacrylamide): experiment, theory and application. *Prog. Polym. Sci.* **1992**, *17*, 163−249.
(61) Walker, P. J.; Mueller, S.; Smirnova, I. Confidence-Interval and Uncertainty-Propagation Analysis of SAFT-type Equations of State. *J. Chem. Eng. Data* **2024**, *69*, 495−508.
(62) Rubinstein, M.; Colby, R. H. *Polymer physics*; Oxford Univ. Press: 2014.
(63) Bharadwaj, S.; Niebuur, B.-J.; Nothdurft, K.; Richtering, W.; Van Der Vegt, N. F. A.; Papadakis, C. M. Cononsolvency of thermoresponsive polymers: where we are now and where we are going. *Soft Matter.* **2022**, *18*, 2884−2909.
(64) Hanwell, M. D.; Curtis, D. E.; Lonie, D. C.; Vandermeersch, T.; Zurek, E.; Hutchison, G. R. Avogadro: An advanced semantic chemical editor, visualization, and analysis platform. *J. Cheminform.* **2012**, *4* (1), 17.
(65) Rehner, P.; Bauer, G.; Gross, J. FeO_s: An Open-Source Framework for Equations of State and Classical Density Functional Theory. *Ind. Eng. Chem. Res.* **2023**, *62*, 5347−5357.

https://doi.org/10.1021/acs.iecr.6c01731
Ind. Eng. Chem. Res. 2026, 65, 16852−16866